Inflamed neutrophils sequestered at entrapped tumor cells via chemotactic confinement promote tumor cell extravasation

Michelle B. Chen[a], Cynthia Hajal[a], David C. Benjamin[b,c], Cathy Yu[d], Hesham Azizgolshani[a], Richard O. Hynes[b,c], and Roger D. Kamm[a,d,e,1]

[a]Department of Mechanical Engineering, Massachusetts Institute of Technology, Cambridge, MA 02139; [b]Department of Biology, Massachusetts Institute of Technology, Cambridge, MA 02139; [c]Koch Institute for Integrative Cancer Research at MIT, Cambridge, MA 02139; [d]Department of Biological Engineering, Massachusetts Institute of Technology, Cambridge, MA 02139; and [e]Howard Hughes Medical Institute, Chevy Chase, MD 20815

Edited by Mina J. Bissell, E. O. Lawrence Berkeley National Laboratory, Berkeley, CA, and approved May 29, 2018 (received for review September 18, 2017)

Systemic inflammation occurring around the course of tumor progression and treatment are often correlated with adverse oncological outcomes. As such, it is suspected that neutrophils, the first line of defense against infection, may play important roles in linking inflammation and metastatic seeding. To decipher the dynamic roles of inflamed neutrophils during hematogenous dissemination, we employ a multiplexed microfluidic model of the human microvasculature enabling physiologically relevant transport of circulating cells combined with real-time, high spatial resolution observation of heterotypic cell–cell interactions. LPS-stimulated neutrophils (PMNs) and tumor cells (TCs) form heterotypic aggregates under flow, and arrest due to both mechanical trapping and neutrophil–endothelial adhesions. Surprisingly, PMNs are not static following aggregation, but exhibit a confined migration pattern near TC–PMN clusters. We discover that PMNs are chemotactically confined by self-secreted IL-8 and tumor-derived CXCL-1, which are immobilized by the endothelial glycocalyx. This results in significant neutrophil sequestration with arrested tumor cells, leading to the spatial localization of neutrophil-derived IL-8, which also contributes to increasing the extravasation potential of adjacent tumor cells through modulation of the endothelial barrier. Strikingly similar migration patterns and extravasation behaviors were also observed in an in vivo zebrafish model upon PMN–tumor cell coinjection into the embryo vasculature. These insights into the temporal dynamics of intravascular tumor–PMN interactions elucidate the mechanisms through which inflamed neutrophils can exert proextravasation effects at the distant metastatic site.

metastasis | inflammation | neutrophils | extravasation | cell migration

To metastasize successfully, tumor cells (TCs) must undergo hematogenous dissemination and extravasation, a process now widely believed to involve both cooperative and antagonistic interactions between host microenvironmental factors and tumor cells (1). In particular, tumor cells encounter a variety of blood cells in circulation, including neutrophils—the predominant circulating granulocyte in humans (2). Currently, the roles of neutrophils in metastatic seeding are controversial (3). Clinical studies have shown that neutrophilia often predict worsened metastasis-specific survival (4). In support of this, neutrophils can enhance metastatic foci formation in experimental mouse models, seen by the decrease in metastatic burden upon their depletion via anti-Ly6G (5–7), or increase when exogenous human neutrophils are added (8, 9). Various mechanisms have been proposed for this prometastatic effect, including the increase in tumor cell retention in the vasculature via tumor–neutrophil adhesions through integrins (8). Neutrophil derived factors such as LTB4 are also thought to enhance colonization by selectively expanding the subpool of cancer cells with high tumorigenic potential (5). Conversely, accumulation of neutrophils in the premetastatic lung can inhibit metastatic seeding by generating H_2O_2, an effect mediated by tumor-secreted CCL2 (10, 11). Thus, neutrophil–tumor cell interactions may not be uniformly prometastatic.

Much attention has been focused on the link between systemic inflammation and metastatic seeding. In particular, tumor treatment courses are often marked by instances of inflammatory activation, which have been correlated with adverse metastatic outcomes independent of the morbidity associated with the inflammatory response itself (12–14). Treatment-associated inflammation can arise from perioperative infections (12, 15) and other curative interventions, including palliative surgery and chemotherapy (sterile inflammation) (14, 16–19). Neutrophils are generally key players in inflammatory responses, with their roles studied in animal models of injury, including cecal ligation and ischemia reperfusion, where the formation of neutrophil extracellular traps (NETs) can trap circulating tumor cells and enhance metastasis (18, 20). Similarly, prestimulation of neutrophils with lipopolysaccharide (LPS) increased tumor cell retention in hepatic sinusoids and gross metastases (9). Combined with the finding that tumor resection often sheds cancer cells into the circulation (21, 22), it is crucial to elucidate the roles of neutrophils in the link between inflammation and distant metastasis.

Using an in vitro model of human microvasculature and LPS-stimulated neutrophils to mimic an inflamed state, we show that the initial intraluminal clustering of TCs and PMNs is dependent on both physical trapping and adhesive interactions between

Significance

Systemic inflammation that occurs during the course of tumor treatment is often correlated with adverse oncological outcomes independent of the infectious insult. As the first line of defense against infection, it is likely that neutrophils play an important role in modulating the progression of distant metastases in these scenarios. This study uses a multiplexed microfluidic model of human microcirculation combined with LPS-stimulated neutrophils as a model of systemic infection to probe the dynamic interactions between intravascular tumor cells and neutrophils at high spatiotemporal resolutions. We uncover chemokine-dependent neutrophil migration patterns which result in enhanced tumor cell extravasation rates. These findings may provide a basis for inhibiting the proextravasation and possibly prometastatic effect of inflamed neutrophils.

Author contributions: M.B.C., D.C.B., R.O.H., and R.D.K. designed research; M.B.C., C.H., D.C.B., and C.Y. performed research; H.A. contributed new reagents/analytic tools; M.B.C., C.H., and C.Y. analyzed data; and M.B.C., C.H., D.C.B., and R.D.K. wrote the paper.

The authors declare no conflict of interest.

This article is a PNAS Direct Submission.

[1]To whom correspondence should be addressed. Email: rdkamm@mit.edu.

This article contains supporting information online at www.pnas.org/lookup/suppl/doi:10.1073/pnas.1715932115/-/DCSupplemental.

Published online June 18, 2018.

PMNs and endothelial ICAM-1. However, after arrest, PMNs within clusters are highly migratory, not maintaining firm contact with TCs. Interestingly, these PMNs migrate in a confined manner mediated by PMN self-secreted IL-8 and tumor-derived CXCL-1, causing them to be sequestered in TC–PMN clusters. Moreover, migratory confinement is enhanced by the endothelial cell (EC) glycocalyx, likely via chemokine immobilization. Strikingly, similar confined migration patterns were observed in the vasculature of an in vivo zebrafish metastasis model. This sequestration of PMNs at the vicinity of tumor cell clusters results in the spatial localization and sequestration of PMN-derived IL-8, leading to endothelial barrier disruption and enhancing the extravasation of nearby entrapped tumor cells.

Results

Intravascular TC–PMN Aggregation Is Modulated by Mechanical Trapping and Adhesive Interactions. Previously, we described and characterized a microfluidics-based, in vitro assay featuring 3D perfusable microvascular networks for studying tumor cell extravasation dynamics (23–25). Precise details on the method of vasculature formation and tumor cell perfusion can be found elsewhere (26). The microdevice features self-organized human microvascular networks formed by human umbilical vein endothelial cells (HUVECs) in fibrin gels, through which TCs can be perfused and extravasation events can be tracked via standard confocal microscopy. Here, we improve upon the existing assay in terms of throughput, robustness of perfusable network formation, and ease of use (Fig. 1*A* and *SI Appendix*, Fig. S1). Upon network formation, continuous flow can be established via an integrated reservoir that applies a passive hydrostatic pressure difference (Fig. 1*B*).

To recapitulate the inflamed phenotype, neutrophils were stimulated with LPS for 30 min, washed three times, followed by coperfusion with A375-MA2 melanoma cells into in vitro vascular beds. After a few minutes of flow, many cells aggregated into heterotypic clusters (Fig. 1*C* and *SI Appendix*, Fig. 2*A*). LPS prestimulation up-regulated surface CD11b expression and subsequently increased the aggregation index of PMNs with TCs (Fig. 1*D* and *SI Appendix*, Fig. S2). It also led to larger clusters and a greater number of PMNs arrested per device, while anti-CD11b attenuated this clustering (*SI Appendix*, Fig. S2*C*). These results suggest the presence of adhesive interactions modulating TC–PMN aggregation. Treatment of vessels or TCs with anti–ICAM-1 alone resulted in less clustering, with blocking of EC–ICAM-1 alone giving a stronger reduction. Interestingly, ICAM-1 expression increased on endothelial cells upon MA2 cell perfusion alone, and even more so with MA2 and stimulated PMN coperfusion (*SI Appendix*, Fig. S3*A*). When tumor cells were substituted with 15-μm beads, ICAM-1 intensity did not increase while TC–PMN aggregation decreased, suggesting that initial endothelial stimulation by tumor cells modulates the CD11b–ICAM-1 adhesions (Fig. 1*D*). Despite the inert nature of the beads, the baseline level of aggregation indicates that mechanical trapping also plays a significant role in clustering. Contrary to our expectations, the addition of PMNs did not increase the initial trapping rate (<5 min) of TCs; however, significant differences were seen in TC retention (>3 h), suggesting that PMNs can enhance TC resistance to shear flow (*SI Appendix*, Fig. S3*B*), increasing the absolute number of cells available to extravasate. Altogether, our data suggest that the degree of initial TC–PMN clustering and the overall PMN retention in the vasculature are dependent on adhesive interactions between neutrophil CD11b and endothelial ICAM-1 up-regulated upon TC and PMN contact, in addition to physical trapping mechanisms. Heterotypic clustering further prevents tumor cell loss from flow.

Clustered PMNs Are Chemotactically Confined by PMN-Derived IL-8 and TC-Derived CXCL-1. Time-lapse imaging of individual "TC–PMN clusters" revealed that clustered PMNs were not static but highly migratory on the surface of the endothelium, with some transmigrating into the surrounding matrix (Movies S1 and S2). PMNs were categorized into two subpopulations—"cluster-associated" or "free"—based on their proximity to arrested clusters (Fig. 2*A* and *SI Appendix*, Fig. S4 *A* and *B*). Cluster-associated PMNs exhibited both decreased migration speeds and end-to-end displacements compared with free PMNs over 90 min (Fig. 2*B*). Strikingly, cluster-associated PMNs remained more confined to their original position, whereas free PMNs exhibited significantly greater dispersion (Fig. 2*C* and Movies S3 and S4).

Cytokine arrays revealed two highly expressed neutrophil chemotactic factors, IL-8 (from MA2 and inflamed PMNs) and CXCL-1 (from MA2) (Fig. 2*D* and *SI Appendix*, Fig. S6*A*), and when neutralized with antibodies in the devices, we observed increased PMN dispersion, migration speed, and displacement (Fig. 2 *E* and *F*), as well as increased separation distance from the periphery of the TC–PMN cluster (*SI Appendix*, Fig. S5 *A* and *B*). PMN dispersion behaviors persisted for as long as 6 h (Fig. 3*A*). Thus, it is likely clustered cells could behave as a concentrated chemokine source for nearby PMNs. We then deciphered the relative levels of contributions of individual chemokines and their sources. While blocking CXCL-1 alone resulted in a significant reduction in dispersion, blocking IL-8 alone produced dispersions at similar levels as coblocking (Fig. 3*B*). This suggests that IL-8 is a more potent chemokine than CXCL-1 in confinement; however, loss of IL-8 may be slightly compensated for by the activity of CXCL-1 or other chemokines. Since IL-8 is secreted by both stimulated PMNs and MA2s at high levels (*SI Appendix*, Fig. S8 *B* and *C*), we decoupled the two sources via siRNA. Interestingly, ablation of tumor-derived IL-8

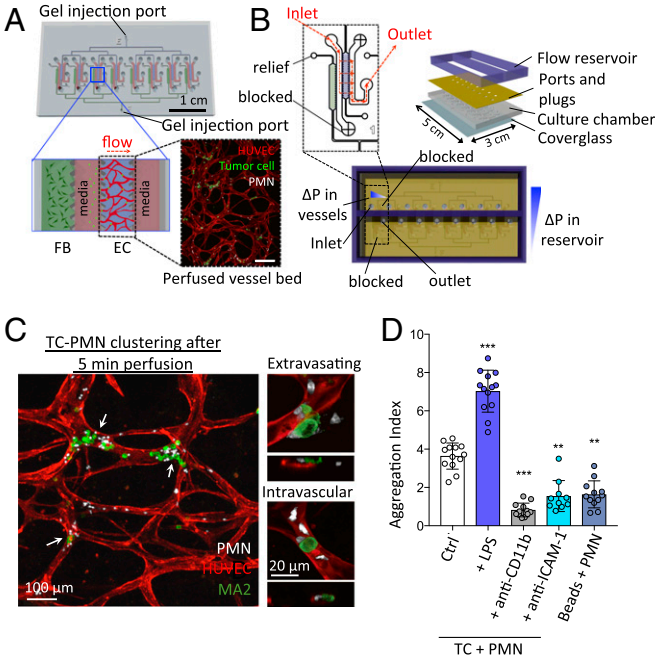

Fig. 1. Multiplexed microvascular network assay allows quantification of TC–PMN arrest and extravasation dynamics. (*A*) Eight independent hydrogel regions where microvascular networks, connected by branching channels, are formed per chip. Fluorescence *Inset* depicts a confocal projection of one perfused vascular network. (Scale bar: 200 μm.) (*B*) A reservoir sustaining a hydrostatic pressure drop of ∼5 mm water is secured on top of the chip to generate continuous perfusion. (*C*) TC–PMN clusters in microvessels. Higher magnification examples of extravasating and nonextravasated MA2 cells in TC–PMN clusters. (*D*) Degree of tumor cell–PMN aggregate formation during intravascular arrest. Aggregation index is defined as the fraction of TCs clustered with neutrophils multiplied by the average number of neutrophils per cluster (n = 10–13 devices per condition). $^{**}P < 0.01$, $^{***}P < 0.001$, and error bars indicate SD.

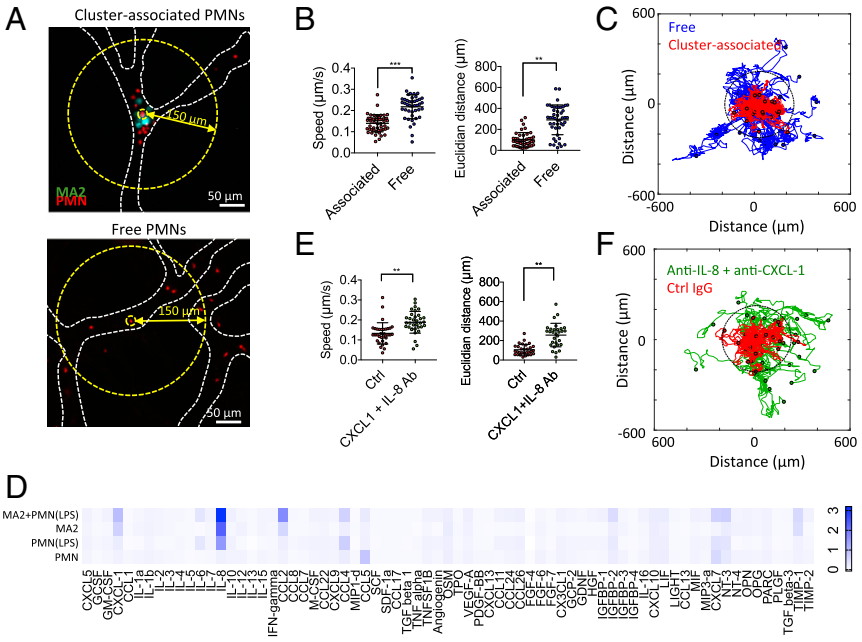

Fig. 2. Cluster-associated PMNs exhibit migratory confinement that is dependent on autologous chemotaxis to secreted factors. (*A*) Cluster-associated and free PMNs arrested intraluminally. (*B*) Migration speeds and end-to-end distance from original position of cluster-associated vs. free PMNs (n = 43–53 PMNs per condition over five devices). (*C*) Tracks of free (blue) and cluster-associated (red) PMNs over 90 min (40-s time step). Dotted circle delineates the 150-μm radius. (*D*) Cytokine array showing relative magnitudes of secreted factors from MA2 alone, PMN alone, LPS-activated PMNs, or MA2 + PMN coincubation, after 4 h of culture (two replicates). (*E*) Migration speed and end-to-end distance from original position of cluster-associated PMNs with or without anti–CXCL-1 + anti–IL-8 (n = 30–34 PMNs per condition, over five devices). Error bars indicate SD, $^{**}P < 0.01$, $^{***}P < 0.001$. (*F*) Migration tracks of cluster-associated PMNs incubated with anti–CXCL-1 + anti–IL-8 or control (Ctrl) IgG.

did not significantly alter neutrophil sequestration (Fig. 3*C*). Replacement of TCs with 15-μm beads produced no changes in dispersion, while treatment of beads and PMNs with anti–IL-8 caused high levels of dispersion, suggesting that PMN self-derived IL-8 is sufficient to induce chemotactic confinement. COMSOL simulations further confirmed that IL-8 gradients could be maintained in the presence of flow (*SI Appendix*, Fig. S9). Moreover, IL-8 secreted by activated PMNs might be sequestered within the glycocalyx that coats the surface of the endothelium. This could help maintain sufficient levels of IL-8 under flow, as shown by significant PMN dispersion from clusters (without changes in migration speed) when vessels are pretreated with heparinase III (Fig. 3*C* and *SI Appendix*, Fig. S10).

Transmigrated extravascular PMNs (which were further categorized into free and cluster-associated populations) exhibited similar dispersion patterns to the respective cases where intra- and extravascular PMNs were not distinguished. In addition, free PMNs were much more likely to extravasate compared with cluster-associated PMNs, while blocking IL-8 and CXCL-1 increased cluster-associated PMN extravasation rates (*SI Appendix*, Fig. S11 and Movie S5). Together, this suggests that differences in

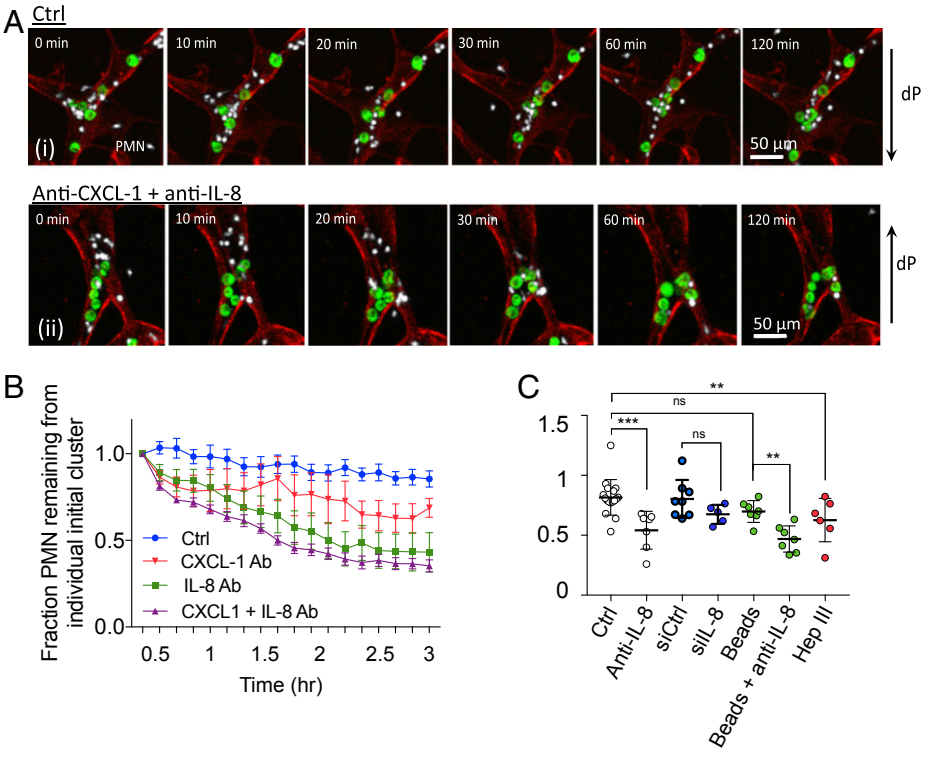

Fig. 3. Confined PMN migration sequesters PMNs near TCs for >6 h, and is enhanced by the endothelial glycocalyx. (*A*) Cluster-associated PMNs and their dispersion from TCs over 2 h, in the absence and presence of anti–CXCL-1 + anti–IL-8. (*B*) Fraction of PMNs remaining in individual clusters over 3 h (every 10 min) when the system is treated with IL-8 and/or CXCL-1 neutralizing antibodies, or when tumor cells are replaced with 15 μm polystyrene beads (n = 15 clusters per group over three independent devices, at each time point). (*C*) Fraction of PMN remaining per TC–PMN cluster at 6 h. Devices are treated with either IgG or anti–IL-8 and/or anti–CXCL-1. In some cases, only tumor-derived IL-8 and/or CXCL-1 is ablated via siRNA. Each point represents one device with at least five TC–PMN clusters averaged per device (n > 5 devices per condition). $^{**}P < 0.01$, $^{***}P < 0.001$, n.s. = not significant, error = SEM.

the availability of adhesion receptors on the endothelium (e.g., ICAM-1) are not modulating PMN confinement.

Thus, after TC–PMN aggregation via trapping and adhesive mechanisms, PMNs are further sequestered by chemotactic confinement mediated by self-derived IL-8 and tumor derived CXCL-1. Chemokine immobilization in the endothelial glycocalyx may further act to enhance the availability of IL-8 and hence migratory confinement.

Spatial Localization of Neutrophils and Their Secreted Factors Promotes Local Tumor Cell Extravasation. Melanomas A375 and A375-MA2 and breast MDA-MB-231 were coperfused with either quiescent or LPS-stimulated PMNs. While systemic injection of LPS induced the highest level of extravasation (*SI Appendix*, Fig. S6*D*), coperfusion with only LPS-prestimulated PMNs also significantly increased extravasation in all three cell lines, indicating a direct effect from stimulated PMNs alone (Fig. 4*A*). Importantly, extravasation rates of PMN-associated cells were higher compared with PMN-free cells, suggesting the presence of a proximity-dependent effect of PMNs on neighboring TCs and/or ECs (Fig. 4*B*). Neutralizing IL-8 not only abrogates PMN sequestering but also decreases the extravasation rates of PMN-associated TCs. There is no effect on extravasation rates of the free subpopulation, indicating a direct correlation between IL-8–dependent migratory confinement and extravasation. Device incubation with conditioned media from stimulated PMNs alone or MA2–PMN coculture produced similar increases in extravasation (Fig. 4*C*). Thus, PMN migratory confinement could facilitate the spatial localization of PMN-derived proextravasation factors to nearby arrested TCs and enhance their transmigration potential.

Coperfusion of unstimulated PMNs also resulted in increased extravasation (although less so) in A375 and MA2, but not MDA-MB-231. Since ICAM-1 expression has been associated with increased malignancy of certain melanomas (27), it is possible that tumor ICAM-1 could autonomously modulate extravasation, and greater expression of ICAM-1 in certain tumor cell lines could lessen the requirement of PMNs and systemic inflammation to extravasate, compared with tumors with lower levels. We tested the extravasation rates of a panel of cell lines including melanomas (A375, A375-MA2, and WM266-4), colon (HT29 and SW620), and nonsmall cell lung cancer (NSCLC) (H2126 and H2087) and their correlation to ICAM-1 surface expression as measured via flow cytometry. In general, extravasation potentials are positively correlated with ICAM-1 levels for the melanoma and NSCLC lines tested, but not colon lines, suggesting tumor-type specificity (*SI Appendix*, Fig. S6*B*). Neutralizing tumor ICAM-1 results in a decrease in MA2 extravasation but not A375 or MDA-MB-231, suggesting that tumor ICAM-1 can modulate extravasation independently of infection, but perhaps only when ICAM-1 is expressed at sufficient levels. Furthermore, while tumor ICAM-1 does enhance the levels of tumor–PMN aggregation and arrest in capillaries, ICAM-1 interaction with PMNs could stimulate protumor cell extravasation effects in PMNs, in the absence of systemic infection. When melanoma ICAM-1 is neutralized in the presence of quiescent PMNs, extravasation rates decrease, but do not reach the levels seen with blocking TC ICAM-1 in the absence of PMNs. Thus, PMNs can exert, at least in part, a proextravasation effect that is not derived from the presence of tumor ICAM-1. Lastly, blocking of ICAM-1 in the presence of MA2 and LPS-stimulated PMNs does not attenuate extravasation, indicating that infection-induced increases in extravasation is not dependent on ICAM-1 (*SI Appendix*, Fig. S6 *C–E*). Thus, it remains clear that regardless of the role of tumor ICAM-1, systemic inflammation dramatically increases extravasation, and ICAM-1 does not appear to play a critical role in this case.

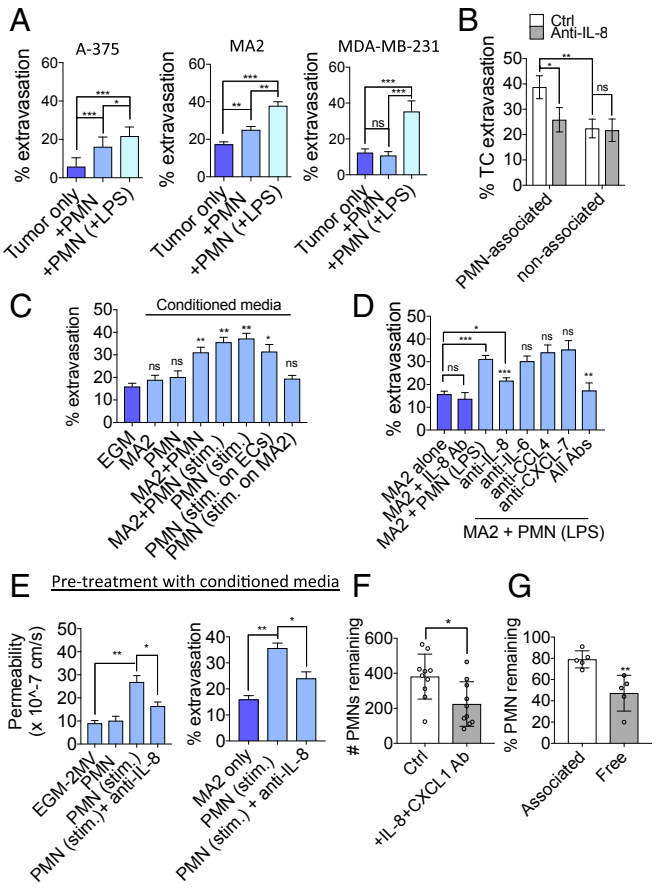

Fig. 4. IL-8 released by LPS-stimulated PMNs increases TC extravasation rates through the action of IL-8 on local EC barrier function. (*A*) Percentage of extravasated cells at 6 h for A375, A375-MA2, and MDA-MB-231 when coperfused with quiescent PMNs or LPS-stimulated PMNs at a 1:5 ratio (n = 12 devices). (*B*) Percentage of MA2 extravasated in the PMN-associated or nonassociated subpopulations within the same device, with or without anti–IL-8 (n = 6 devices). (*C*) Extravasation rates of MA2 at 6 h when coincubated with conditioned media (CM) generated from various conditions (n > 9 devices per condition). (*D*) Extravasation rates of MA2 in the presence of stimulated PMNs and neutralizing antibodies at 6 h postinjection (n = 5 devices). (*E*) Permeability of microvessels to 70 kDa dextran after 6-h treatment with stimulated PMN conditioned media. Extravasation rates (at 6 h) of MA2 tumor cells in PMN-conditioned media pretreated vessels (for 6 h) (n = 3 devices). (*F*) Percentage of original (at t = 0) PMNs remaining in microvessel beds after 6 h of flow in the absence or presence of anti–IL-8 + anti–CXCL-1 (n = 10 devices). (*G*) Percentage of PMNs remaining in cluster-associated or free subpopulations after 6 h of flow (with MA2 coperfusion). Each point represents the average of at least five clusters across five regions of interest (ROIs), or at least 20 free PMNs over five ROIs. In *A–G*, error bars indicate SEM, $*P < 0.05$, $**P < 0.01$, $***P < 0.001$.

PMN-Derived IL-8 Plays Multiple Roles in PMN Sequestration and Enhancing Tumor Cell Extravasation. Out of the cytokines upregulated upon PMN stimulation with LPS stimulation or coincubation with MA2s (IL-8, IL-6, CCL4, and CXCL-7), only blocking of IL-8 reduced transmigration (Fig. 4*D*). Device treatment with PMN-conditioned media increased extravasation, while coincubation of conditioned media with anti–IL-8 attenuated this response, indicating that PMN-derived IL-8 is responsible for enhancing extravasation in a contact-independent manner (Fig. 4*E*). This is also correlated with an increase in vascular permeability when vessels are pretreated with PMN-conditioned media, which is attenuated with anti–IL-8 (Fig. 4*E*).

Since MA2 produced IL-8 to a similar extent as stimulated PMNs, we asked whether IL-8 solely derived PMNs could be

sufficient to enhance extravasation, regardless of tumor-derived IL-8 levels. Coperfusion of IL-8 siRNA-treated MA2 and LPS-stimulated PMNs did not attenuate extravasation rates (*SI Appendix*, Fig. S8), indicating that MA2-derived IL-8 alone may be below the threshold level to induce appreciable consequences in transmigration. Thus, beyond modulating chemotactic confinement, PMN-derived IL-8 could play an additional role in facilitating extravasation via perturbation of endothelial barrier function.

Lastly, increased dispersion of PMNs from clusters is correlated with a loss of PMNs from the entire microvascular bed (Fig. 4*F*). Loss of free PMNs was significantly higher compared with PMNs that were originally cluster associated, suggesting that sequestered PMNs are more protected from shear flow (Fig. 4*G*). Thus, migratory confinement of PMNs at clusters may enhance the numbers of PMNs arrested in the microvasculature and maximize the proextravasation effect of PMNs.

Inflamed PMNs Exhibit Confined Migration and Enhance Tumor Cell Extravasation in Zebrafish Embryos. Similar to the on-chip vascular model, when LPS-stimulated neutrophils are coinjected with A375 or MA2 in zebrafish embryos, PMNs rapidly arrest in heterotypic aggregates, and most remain lodged for periods of >6 h (*SI Appendix*, Fig. 5*A* and Movie S6). Remarkably, we observed similar confinement behavior of cluster-associated PMNs compared with free PMNs (Fig. 5*B*). Unlike the on-chip model, neutrophils continue to circulate throughout the embryo over time. Despite this, we observed very few neutrophils to be recruited to existing clusters over time, as the occlusion of the vessel appears to prevent significant further blood flow into the vicinity. Lastly, we confirmed that coinjection of both MA2s and A375 with stimulated human PMNs increased tumor cell extravasation rates over a period of 12 h, similar to our results obtained in vitro (Fig. 5*C*).

Discussion

While the roles of neutrophils at the primary tumor site have been extensively studied, whether neutrophils play pro- or antimetastatic functions during hematogenous dissemination is less clear. Inflammatory activation during the course of tumor progression may arise from infections from curative interventions like resection surgeries (18), sterile inflammation from chemotherapy (19), and even conditioning by the primary tumor itself (3). Importantly, inflammation is often correlated with adverse oncological outcomes independent of the morbidity associated with inflammatory response (12–14). Thus, neutrophils may play an important role in linking infection, inflammation, and metastasis. In this study, we sought to understand the dynamic roles of inflamed neutrophils during tumor cell arrest and extravasation.

We employ an in vitro model of the human microvasculature, enabling us to dynamically visualize tumor–PMN–endothelial interactions at high spatiotemporal resolutions that would otherwise be challenging in vivo. We are able to recapitulate key events such as the arrest of tumor cells and neutrophils in vessels with diameters and flow patterns comparable to those of in vivo microvasculature (23, 24). This is key since TC–PMN clustering, PMN sequestration, and the formation of chemokine gradients cannot be recapitulated in static assays or those involving flow over a flat endothelial layer. Furthermore, the thin height of our tissues (<150 μm) facilitates tracking of rapidly migrating neutrophils compared with imaging in thick tissues in vivo. This allows us to determine the spatial relationships between single cells and resolve the different migratory behaviors between cell subpopulations, such as neutrophil autologous chemotaxis at trapped clusters.

It has been previously shown in mouse models of dissemination that arrested tumor cells can colocalize with neutrophils through integrins (8, 9, 28, 29), NETs (18), or the attraction of platelets (7). Dong and coworkers (8) showed that tumor cell ICAM-1 and PMN CD11b/beta-2 facilitated TC-PMN aggregation within a parallel flow chamber. However, realistically, TCs and PMNs interact in narrow capillaries (rather than a flat surface) where physical occlusion and increased contact area with the endothelium may play a role. By coupling both mechanisms in our assay, we further discover that the up-regulation of endothelial ICAM-1 upon contact with TCs and PMNs can enhance association rates and yields a stronger effect than tumor ICAM-1. Importantly, physical occlusion can play a significant role in TC–PMN clustering, as substituting PMNs with 4-μm beads in microvessels still leads to nontrivial levels of TC–bead association.

Initial TC–PMN clustering under flow may be an important prerequisite for the chemotactic sequestration of PMNs. Rather than forming stable adhesions to TCs postarrest, cluster-associated neutrophils migrate in a "back and forth" motion within an ~70-μm radius of the original TC–PMN cluster, via a migratory confinement mechanism that is dependent on PMN-derived IL-8. Interestingly, this behavior exists even without appreciable neutrophil recruitment from other parts of the vascular bed, as the initial levels of PMNs in clusters formed during intravascular arrest are likely sufficient to establish a chemokine source.

Confinement of PMNs at arrested tumor clusters may be key in enhancing the proextravasation effects of PMNs. Inflamed PMNs secrete high levels of IL-8, which, in addition to mediating migratory confinement, can further disrupt the endothelial barrier, facilitating the transmigration of tumor cells. Furthermore, while MA2 also secretes IL-8, it appears that the majority of the proextravasation effect of IL-8 arises from PMNs alone. The PMN-associated subpopulation of TCs exhibits markedly higher extravasation rates, suggesting proximity-dependent effects of PMNs on extravasation. It is likely that the sequestration of PMNs at arrested tumor foci allows IL-8 to be highly localized and act effectively on the adjacent endothelium. The significant increase in the number of colocalized PMNs per tumor cluster upon LPS treatment could further exacerbate this effect. Furthermore, extravasation rates in PMN-associated TCs decreased upon neutralization of chemotactic factors IL-8 and CXCL-1,

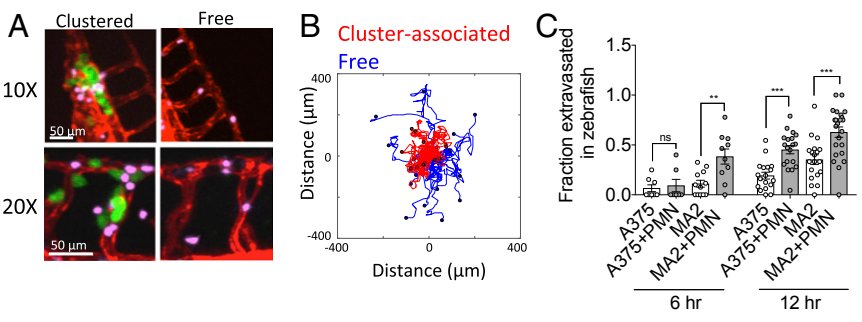

Fig. 5. Inflamed PMNs are sequestered at TC–PMN clusters and enhance extravasation rates of A375 and MA2 in vivo. (*A*) Intravascular cluster-associated and free PMNs (pink) when coinjected with MA2 cells (green) in flk:dsRed (red) zebrafish embryos. (*B*) Migration tracks of cluster-associated or free PMNs in vessels of zebrafish embryos. (*C*) Extravasation rates of A375 and MA2 cells with or without coperfusion with inflamed PMNs at 6 h and 24 h (n = 7–12 embryos for A375, n = 18–23 embryos for MA2). Error bars indicate SEM, $^{**}P < 0.01$, $^{***}P < 0.001$.

but not in the nonassociated population, indicating that PMN confinement is critical for the effects of PMN-derived IL-8 to be exerted. In fact, melanoma IL-8 has been implicated in VE-cadherin dissasembly (30). While we have also found IL-8 to be the key effector in our system, our study implicates PMN-derived IL-8 (rather than TC-derived) and the direct effect of its sequestration near tumor cells on facilitating tumor cell transendothelial migration.

We use LPS-stimulated neutrophils to mimic the inflamed phenotype that would be typically found during infection-induced inflammation. However, the inflamed state of neutrophils can be heterogeneous depending on the source of inflammatory stimulus (e.g., sterile inflammation, conditioning from a primary tumor). Interestingly, even without prestimulation, PMNs are still capable of elevating tumor cell extravasation rates (albeit to a lesser degree than stimulated PMNs). Thus, tumor cells may possess the ability to activate PMNs to produce proextravasation factors (8) which is independent of infection. This is highly likely in instances of sterile inflammation or where neutrophils are conditioned by primary tumors. To support this, PMNs prestimulated with tumor-conditioned media also enhance extravasation. Regardless, PMNs activated by infection may promote extravasation to a much greater extent than the effects of tumor cells alone, and appear to do so without tumor cell-type specificity.

Using an in vitro model of human microvasculature, we show that inflamed PMNs and tumor cells can arrest in heterotypic clusters due to mechanical trapping in narrow capillaries combined with adhesion formation between PMNs and endothelial ICAM-1 up-regulated upon tumor cell perfusion. Cluster-associated PMNs do not form permanent contacts with TCs or ECs, but rather migrate in a confined manner that is mediated by autologous chemotaxis toward self-derived IL-8 and is enhanced by the presence of the EC glycocalyx. Consequently, PMNs are sequestered, resulting in the spatial localization of PMN-derived IL-8, which plays additional roles in disrupting endothelial barrier disruption and enhancing the extravasation potential of nearby arrested tumor cells (*SI Appendix*, Fig. S13).

Materials and Methods

Device Design and Fabrication. The microfluidic chip employed is a higher throughput version of our previous design (23) which serves to advance throughput and robustness and consistency of microvascular network formation. A single gel injection port allows the parallel distribution of cells into eight independent vascular beds through a branching network (Fig. 1*A* and *SI Appendix*).

Zebrafish Embryo Extravasation Assay. Anesthetized embryos (*flk:dsRed2* line crossed into the *casper* background) were injected with 4 nL of 4×10^4 tumor cells per microliter in PBS or 4×10^4 tumor cells and 2×10^5 human LPS-prestimulated PMNs per microliter in PBS. Embryos were placed in a single well of a six-well, glass-bottomed plate (MatTek) containing a thin layer of 2% agarose, and covered in 0.8% agarose containing 0.01% tricaine buffered to pH 7.4. Embryos were imaged on an A1R inverted confocal microscope (Nikon) using the resonant scanner with a 10× objective and 1.5× zoom.

Human Neutrophil Isolation. Human neutrophils were obtained from fresh human blood (diluted 1:1 in HBSS; Invitrogen) purchased from Research Blood Components, which was drawn following the American Association of Blood Banks guidelines. Subjects consist of healthy males and females between the ages of 18 and 65. An institutional review board approved consent form was obtained from each donor, giving permission to use their samples for research purposes. PMNs were isolated using a traditional Histopaque 1077 (Sigma) gradient.

Statistics. Statistical analysis was performed with SigmaPlot using the Student's two-tailed *t* test when comparing two conditions or one-way ANOVA with Tukey's post hoc analysis when applicable.

1. Labelle M, Hynes RO (2012) The initial hours of metastasis: The importance of cooperative host-tumor cell interactions during hematogenous dissemination. *Cancer Discov* 2:1091–1099.
2. Mantovani A, Cassatella MA, Costantini C, Jaillon S (2011) Neutrophils in the activation and regulation of innate and adaptive immunity. *Nat Rev Immunol* 11:519–531.
3. Coffelt SB, Wellenstein MD, de Visser KE (2016) Neutrophils in cancer: Neutral no more. *Nat Rev Cancer* 16:431–446.
4. Noh H, Eomm M, Han A (2013) Usefulness of pretreatment neutrophil to lymphocyte ratio in predicting disease-specific survival in breast cancer patients. *J Breast Cancer* 16:55–59.
5. Wculek SK, Malanchi I (2015) Neutrophils support lung colonization of metastasis-initiating breast cancer cells. *Nature* 528:413–417.
6. Coffelt SB, et al. (2015) IL-17-producing γδ T cells and neutrophils conspire to promote breast cancer metastasis. *Nature* 522:345–348.
7. Labelle M, Begum S, Hynes RO (2014) Platelets guide the formation of early metastatic niches. *Proc Natl Acad Sci USA* 111:E3053–E3061.
8. Huh SJ, Liang S, Sharma A, Dong C, Robertson GP (2010) Transiently entrapped circulating tumor cells interact with neutrophils to facilitate lung metastasis development. *Cancer Res* 70:6071–6082.
9. Spicer JD, et al. (2012) Neutrophils promote liver metastasis via Mac-1-mediated interactions with circulating tumor cells. *Cancer Res* 72:3919–3927.
10. Granot Z, et al. (2011) Tumor entrained neutrophils inhibit seeding in the premetastatic lung. *Cancer Cell* 20:300–314.
11. Granot Z, Jablonska J (2015) Distinct functions of neutrophil in cancer and its regulation. *Mediators Inflamm* 2015:701067.
12. Lin JK, et al. (2011) The influence of fecal diversion and anastomotic leakage on survival after resection of rectal cancer. *J Gastrointest Surg* 15:2251–2261.
13. Auguste P, et al. (2007) The host inflammatory response promotes liver metastasis by increasing tumor cell arrest and extravasation. *Am J Pathol* 170:1781–1792.
14. Schussler O, et al. (2006) Postoperative pneumonia after major lung resection. *Am J Respir Crit Care Med* 173:1161–1169.
15. Andalib A, Ramana-Kumar AV, Bartlett G, Franco EL, Ferri LE (2013) Influence of postoperative infectious complications on long-term survival of lung cancer patients: A population-based cohort study. *J Thorac Oncol* 8:554–561.
16. Shaw C, et al. (2013) Palliative venting gastrostomy in patients with malignant bowel obstruction and ascites. *Ann Surg Oncol* 20:497–505.
17. Feller-kopman D, Berkowitz D, Boiselle P, Ernst A (2007) Large-volume thoracentesis and the risk of reexpansion pulmonary edema. *Ann Thorac Surg* 84:1656–1661.
18. Cools-Lartigue J, et al. (2013) Neutrophil extracellular traps sequester circulating tumor cells and promote metastasis. *J Clin Invest* 123:3446–3458.
19. Vyas D, Laput G, Vyas AK (2014) Chemotherapy-enhanced inflammation may lead to the failure of therapy and metastasis. *OncoTargets Ther* 7:1015–1023.
20. Tohme S, et al. (2016) Neutrophil extracellular traps promote the development and progression of liver metastases after surgical stress. *Cancer Res* 76:1367–1380.
21. Guller U, et al. (2002) Disseminated single tumor cells as detected by real-time quantitative polymerase chain reaction represent a prognostic factor in patients undergoing surgery for colorectal cancer. *Ann Surg* 236:768–776.
22. Liu Z, Jiang M, Zhao J, Ju H (2007) Circulating tumor cells in perioperative esophageal cancer patients: Quantitative assay system and potential clinical utility. *Clin Cancer Res* 13:2992–2997.
23. Chen MB, Whisler JA, Jeon JS, Kamm RD (2013) Mechanisms of tumor cell extravasation in an in vitro microvascular network platform. *Integr Biol* 5:1262–1271.
24. Chen MB, Lamar JM, Li R, Hynes RO, Kamm RD (2016) Elucidation of the roles of tumor integrin ss1 in the extravasation stage of the metastasis cascade. *Cancer Res* 76:2513–2524.
25. Spiegel A, et al. (2016) Neutrophils suppress intraluminal NK cell-mediated tumor cell clearance and enhance extravasation of disseminated carcinoma cells. *Cancer Discov* 6:630–649.
26. Chen MB, et al. (2017) On-chip human microvasculature assay for visualization and quantification of tumor cell extravasation dynamics. *Nat Protoc* 12:865–880.
27. Johnson JP, Stade BG, Holzmann B, Schwable W, Riethmuller G (1989) De novo expression of intercellular-adhesion molecule 1 in melanoma correlates with increased risk of metastasis. *Proc Natl Acad Sci USA* 86:641–644.
28. Zhang P, Goodrich C, Fu C, Dong C (2014) Melanoma upregulates ICAM-1 expression on endothelial cells through engagement of tumor CD44 with endothelial E-selectin and activation of a PKCα-p38-SP-1 pathway. *FASEB J* 28:4591–4609.
29. Zhang P, Ozdemir T, Chung C-Y, Robertson GP, Dong C (2011) Sequential binding of αVβ3 and ICAM-1 determines fibrin-mediated melanoma capture and stable adhesion to CD11b/CD18 on neutrophils. *J Immunol* 186:242–254.
30. Khanna P, Chung C-Y, Neves RI, Robertson GP, Dong C (2014) CD82/KAI expression prevents IL-8-mediated endothelial gap formation in late-stage melanomas. *Oncogene* 33:2898–2908.